



The Use of Electrical Resistivity Tomography to Classify the Earth's Subsurface in Ugbojiobo Community, Edo State, South-South Nigeria

O. J. Airen^{1, *}, M. O. Ekoragbon¹

¹Department of Physics, Faculty of Physical Sciences, University of Benin, Edo State, NIGERIA.

Abstract

Electrical Resistivity investigations using Two-dimensional (2-D) geophysical investigation was carried out in Ugbojiobo community, Ovia North East Local Government Area of Edo State, Nigeria. This was done to have a good idea of subsurface lithology in the study area. Twenty-four (24) traverse lines were profiled in two locations using a rectangular grid format with electrode spacing of 10 m with a horizontal length of 300 m and 200 m respectively using the Wenner Alpha configuration as a survey technique. The 2-D Electrical Resistivity data was processed using RES2DINV software. From the results obtained it is evident that over a depth of between 5 m to 56 m for all the profiled lines there is composition of Alluvium and clayey soil at the top surface with low resistivity values at a depth below 10 m with resistivity values ranging between 50 Ωm –800 Ωm . While Shale, Slate and Sandstone occurred at a depth of between 13 m to 25 m with resistivity values ranging between 1000 Ωm –3000 Ωm . Above a depth of 30 m revealed limestone and thick clay with resistivity values ranging between 5000 Ωm – 30000 Ωm .

Keywords: Profiled, wenner alpha, clayey soil. RES2DINV, traverse, electrode spacing

1.0 INTRODUCTION

The purpose of electrical surveys is to determine the subsurface resistivity distribution by making measurements on the surface. From these measurements, the true resistivity of the subsurface can be estimated. The ground resistivity is related to various geological parameters such as the mineral and fluid content, porosity and degree of water saturation in the rock.

Subsurface resistivity distributions are measured by applying electrical current into the ground by using two current electrodes. The potential differences caused by the flow of current between any two points in linear line with the current electrodes are then measured by a pair of potential electrodes. From the measured voltage (V) and current (I) values, the resistance at the specified point in the subsurface can be determined.

Electrical Resistivity Tomography survey has been widely used in order to solve engineering, archaeological, environmental and geological problems in the last decades. The electrical resistivity surveying method has undergone dramatic changes over the last two decades. direction, so the greatest limitation of one-dimensional (1-D) resistivity

sounding method is that it does not take into account horizontal changes in the subsurface resistivity. A major improvement since the early 1990's is the development of two-dimensional (2-D) imaging surveys that provides a more realistic model of the subsurface even in complex geological area. As we know, due to anisotropy of the earth material, the resistivity changes in x, y and z. A more accurate model of the subsurface is the 2-D model where the resistivity changes in the vertical direction as well as in the horizontal direction along the survey line is put into consideration.

Several electrical properties of rocks and minerals are significant in geoelectrical investigations. They are electrical potentials, electrical resistivity and the dielectric constant. Electrical resistivity array is the most important of these, it is the most applied and used method. Current can be made to flow by direct injection, by capacitive coupling or by electromagnetic induction. Electric Current Surveys, involving direct injection via electrodes at the ground surface are generally referred to as direct current or DC surveys, even though in practice the direction is reversed at regular intervals to cancel some forms of natural background noise.

[1] inverted the 2D apparent resistivity data they collected in Benin City, Edo State, into 3D dataset and subsequently applied the 3D dataset in their geoelectrical

*Corresponding author (Tel: +234 (0) 8039591347)

Email addresses: osariere.airen@uniben.edu (O. J. Airen) and moekhoragbon@gmail.com (M. O. Ekoragbon)

resistivity imaging to determine the effectiveness of using parallel or orthogonal sets of 2D profiles to generate 3D dataset for resistivity imaging. Their result demonstrated that the resolution of the inverted images can be enhanced by using closely spaced 2D profiles or orthogonal 2D profiles. [2] carried out a study to show that a single-channel tetramer can be used to obtain a 3D model of the subsurface. They carried out a 3-Dimensional Electrical Resistivity Tomography (ERT) survey in a basement complex terrain using a 49-electrode system in three locations, with location marked into 7 by 7 square grids with units electrode spacing of 1.0m, 3.0m and 5.0m alongside with pole-pole electrode array.

[3] utilized the 2D and 3D resistivity imaging methods to produce images of the subsurface structure of the University of Technology in Baghdad, Iraq. Three 2D images are utilized to create a 3D slice image and a 3D block image for three conventional arrays. Each 2D image has a length of 60 m and a depth of approximately 12m. The result indicated that the study area consists of two types of material: sandy gravel and clay. The borehole data obtained near the study area confirm the results. The 2D and 3D images, as well as the three conventional arrays, are compared. Wenner array is found to be the most suitable array for 2D and 3D imaging of the study area.

[4] carried out eight parallel two-dimensional (2D) geo-electrical resistivity profiles in hard-rock (Pulivendla) area of Andhra Pradesh, India using a Lund imaging multi-electrode system adopting Wenner array with the aim of evaluating the effectiveness of using parallel 2D profiles for three-dimensional (3D) geo-electrical resistivity imaging for better understanding of aquifer geometry and its characteristics. The results, which are consistent with numerical evaluation, show that high resolution 3D geoelectrical resistivity imaging can be successfully conducted using parallel 2D profiles if appropriate survey parameters are carefully chosen.

2.0 LOCAL GEOLOGY OF THE STUDY AREA

The study was carried out in Ugbogiobo in Ovia Northeast Local Government Area of Edo State, South South Nigeria. Ovia Northeast local government area is one of the eighteen local government areas in Edo State of Nigeria. The local government area was created from the district council under the local government law in 1976. The geological setting in the area of study consists of the coastal plain sands sometimes referred to as Benin sands of the Benin Formation in Nigeria. The Benin sands are partly marine, partly deltaic and partly lagoonal [5], all indications of a shallow water environment of deposition [6]. Benin City is underlain by sedimentary formation [7]. The formation is made up of top reddish clayey sand

capping highly porous fresh water bearing loose pebbly sands, and sandstone with local thin clays and shale interbeds which are considered to be of braided stream origin. Sands, sandstones and clays vary in colour from reddish brown to pinkish yellow on weathered surfaces to white in the deeper fresh surfaces. Limonitic coatings are responsible for the brown reddish-yellowish colour. The formation is covered with loose brownish sand (quaternary drift) varying in thickness and is about 800 m thick; almost all of which is water bearing with water level varying from about 20 m to 52 m [8]. The coastal plain sands in the study area is bounded by Alluvium and Mangrove swamps before it, and afterwards by the Bende Ameki Formation and Imo clay-shale group. The Benin formation encapsulates sedimentary rocks of ages between Palaeocene to recent and contains about 90% of sandstone and shale intercalation. It is coarse grained locally fine grained in some areas, poorly sorted, subangular to well-rounded and bears lignite streaks and wood fragment [9], [10].

3.0 THEORY

In the electrical resistivity method, artificially generated electric currents are introduced into the ground and the resulting potential differences are measured at the surface. Deviations from the pattern of potential differences expected from homogeneous ground provide information on the form and electrical properties of subsurface in homogeneities [11].

The resistivity of a material is defined as the resistance in ohms between the opposite faces of a unit cube of the material.

For a conducting cylinder of resistance δR , length δL and cross-sectional area δA as illustrated in Figure 1 the resistivity ρ is expressed by equation 1

$$\rho = \frac{\delta R \delta A}{\delta L} \quad (1)$$

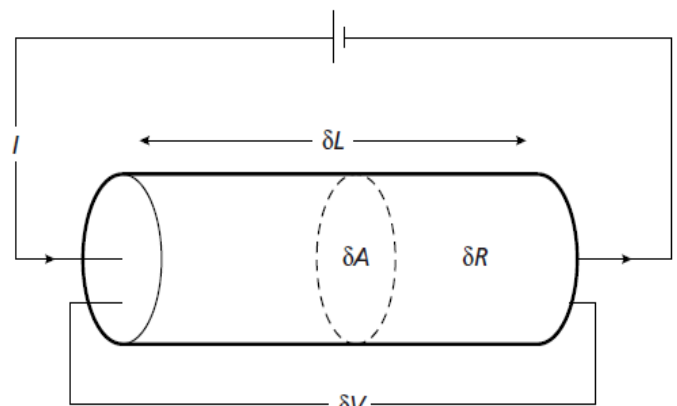


Figure 1: Parameters used in defining resistivity [11].

The SI unit of resistivity is ohm-metre (Ωm) and the reciprocal of resistivity is termed conductivity (units: Siemens (S) per metre; $1\text{Sm}^{-1}=1\ \Omega\text{m}^{-1}$).

Consider the element of homogeneous material shown in Figure 1. A current I is passed through the cylinder causing a potential drop $-\delta V$ between the ends of the element. $\frac{\delta V}{\delta L}$ represents the potential gradient through the element in voltm^{-1} and i the current density in Am^{-2}

$$\frac{\delta V}{\delta L} = \frac{\rho I}{\delta A} = -\rho i \tag{2}$$

In general, the current density in any direction within a material is given by the negative partial derivative of the potential in that direction divided by the resistivity $\frac{\delta V}{\delta L}$ represents the potential gradient through the element in voltm^{-1} and i the current density in Am^{-2} .

Now consider a single current electrode on the surface of a medium of uniform resistivity ρ as shown in Figure 2. The circuit is completed by a current sink at a large distance from the electrode. The current flows radially away from the electrode so that the current distribution is uniform over hemispherical shells centred about the source. At a distance from the electrode the shell has a surface area of $2\pi r^2$, so the current density is given by:

$$i = \frac{I}{2\pi r^2} \tag{3}$$

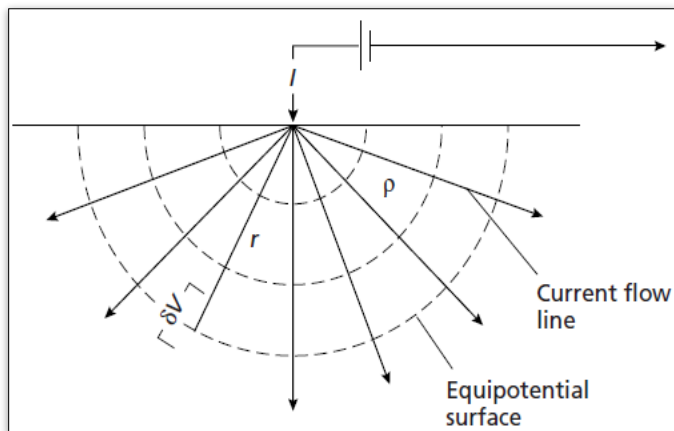


Figure 2: Current flow from a single surface electrode [11].

From equation 2, the potential gradient associated with this current density in equation 3 can be written as shown in equation 4:

$$\frac{\delta V}{\delta r} = -\rho i = -\frac{\rho I}{2\pi r^2} \tag{4}$$

The potential V_r at distance r is then obtained by integration of equation 2.4:

$$V_r = \int \delta V = - \int \frac{\rho I \delta r}{2\pi r^2} = \frac{\rho I}{2\pi r} \tag{5}$$

The constant of integration is zero since $V_r = 0$ when $r = \infty$. Equation 5 allows the calculation of the potential at any point on or below the surface of a homogeneous half-space. The hemispherical shells in Figure 2 mark surfaces of constant voltage and are termed equipotential surfaces.

4.0 METHODOLOGY

- The data was acquired using the following equipment and accessories;
- PASI Terrameter 16GL model
- Thirty-one metal electrodes
- Four hammers for driving the electrodes in the ground
- Crocodile clips
- Two measuring tapes for measuring the distances for the different electrode spacing
- Global Positioning System 72 (GPS) for finding the position and elevation of the survey point
- Power supply- 12V 60Ah battery
- Umbrella
- Four reels of 2 blue and 2 red colored electric cable
- Base map and
- Data sheet for recording the field data

5.0 DATA PROCESSING/INTERPRETATION

The apparent resistivity values for each traverse were collated in a format that is acceptable by the RES2DINV inversion code. Elevation corrections were not included in the measurements as the area surveyed was more or less flat. RES2DINV computer code was used in the inversion of the 2D data. The computer program uses a nonlinear optimization technique which automatically determines a 2D resistivity model of the subsurface for the input apparent resistivity data [12]; [13]. The program divides the subsurface into a number of rectangular blocks according to the spread of the observed data.

Least-squares inversion with standard least-squares constraint which attempt to minimize the square of the difference between the observed and the calculated apparent resistivity values was used to invert all the 2D traverses. The smoothness constraint was applied to the

model perturbation vector only. The sensitivity values provide information on the section of the subsurface with the greatest effect on the measured apparent resistivity values. The sensitivity values were normalized by dividing the calculated sensitivity values with the average sensitivity for the particular model configuration. Line search which uses quadratic interpolation to find the optimum step size for the change in apparent resistivity of model blocks was used at each iteration step. Standard Gauss-Newton optimization method was used, with a convergent limit of 0.005. The Jacobian matrix was recalculated for all iterations; homogeneous half-space was used as initial model. A grid size of 4 nodes per unit electrode and normal mesh were used in the forward modelling subroutine for calculating apparent resistivity values. The initial and minimum damping factor used for the inversion is 0.225 and 0.05, respectively (the default setting is 0.160 and 0.015, respectively). The damping

factor was allowed to increase with depth by a factor of 1.05 since the resolution of resistivity decreases exponentially with depth. The damping factor was optimized so as to significantly reduce the number of iterations required for convergence, however, the time taken per iteration increases.

6.0 RESULTS AND DISCUSSION

The 2D Electrical Resistivity models are shown in Figures 3 to 26. In this model, the results are presented in a color-coded presentation form consisting of the Inverted 2D Resistivity structure obtained from the study area. The horizontal scale on the section is the lateral distance while the vertical scale is the depths, which are both in meters. A minimum to maximum spread of 200 m to 300 m were modelled with the corresponding depth of 39.4 m to 57.3 m investigated on all the profiles as show from Figures 3 to 26.

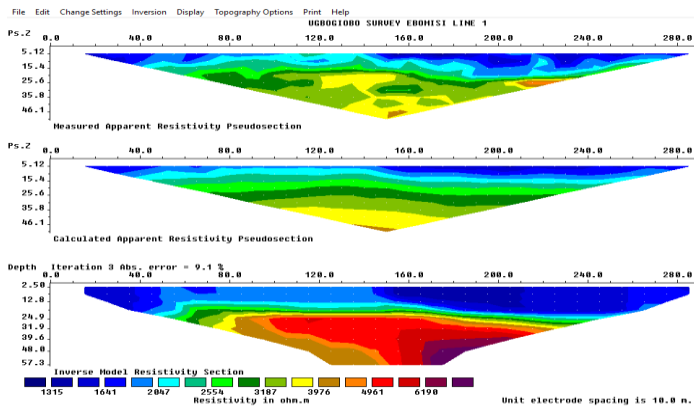


Figure 3: Inverted 2-D resistivity imaging model obtained from Ugbogiobo community profile one

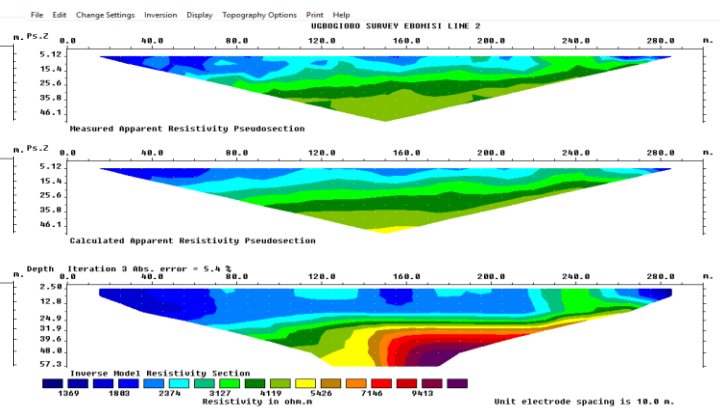


Figure 4: Inverted 2-D resistivity imaging model obtained from Ugbogiobo community profile two.

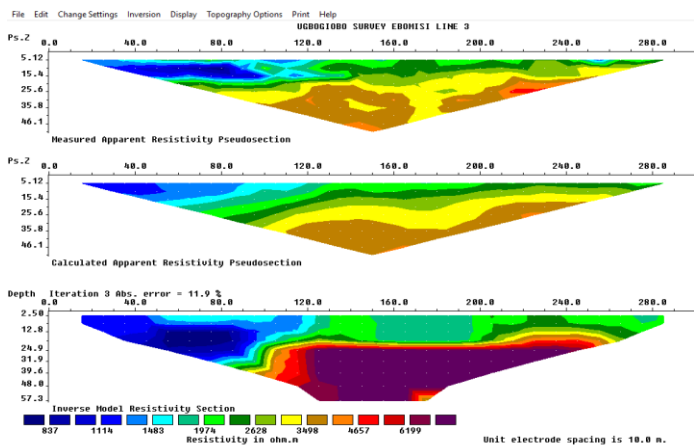


Figure 5: Inverted 2-D resistivity imaging model obtained from Ugbogiobo community profile three

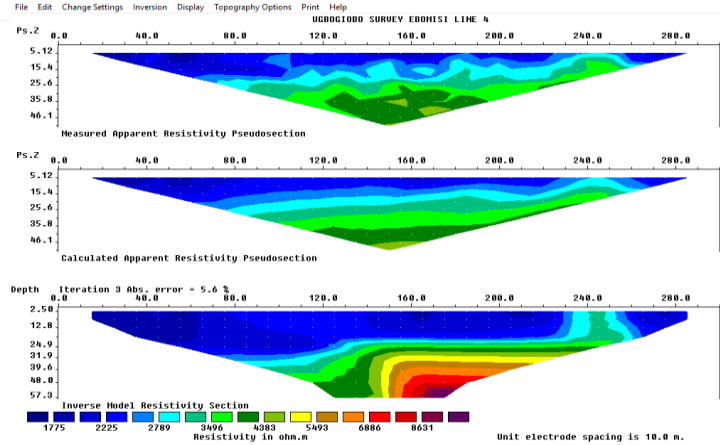


Figure 6: Inverted 2-D resistivity imaging model obtained from Ugbogiobo community profile four

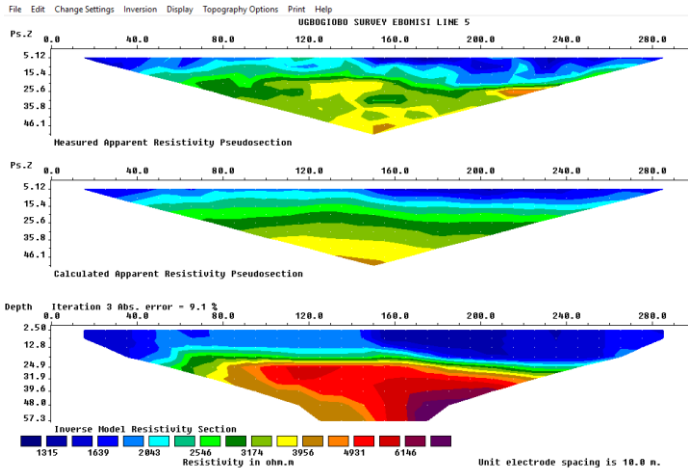


Figure 7: Inverted 2-D resistivity imaging model obtained from Ugbogiobo community profile five

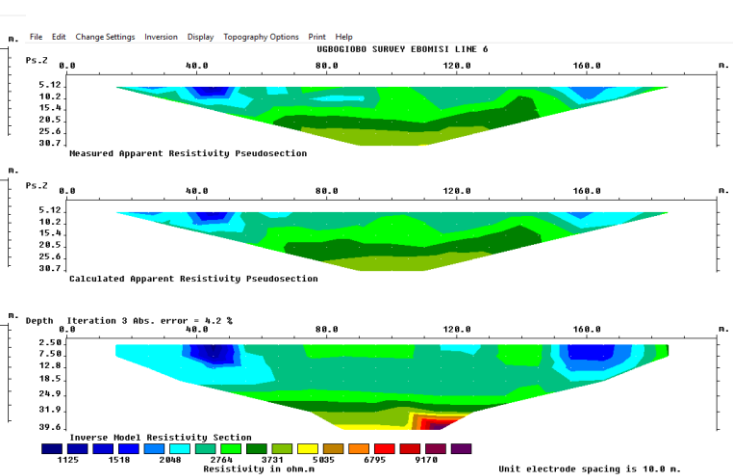


Figure 8: Inverted 2-D resistivity imaging model obtained from Ugbogiobo community profile six

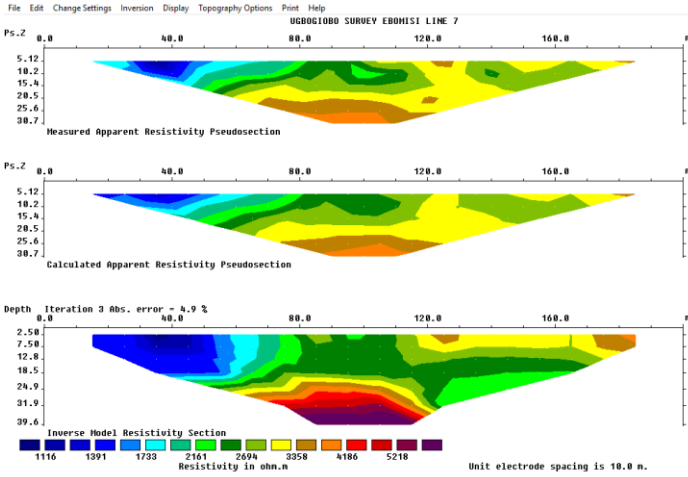


Figure 9: Inverted 2-D resistivity imaging model obtained from Ugbogiobo community profile eight

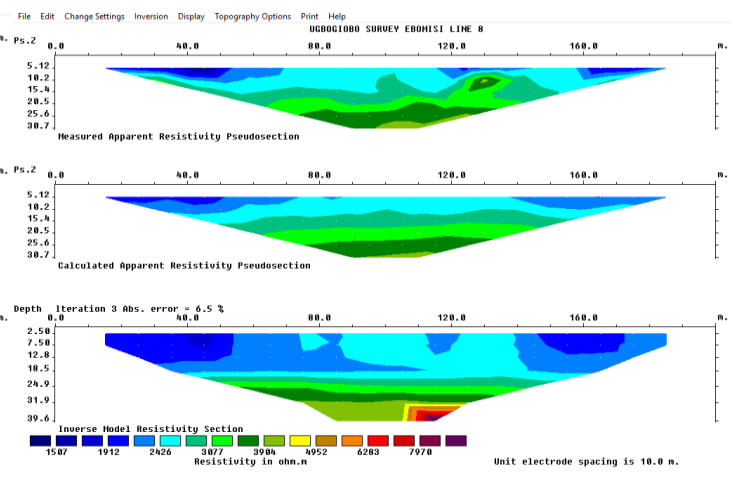


Figure 10: Inverted 2-D resistivity imaging model obtained from Ugbogiobo community profile eight

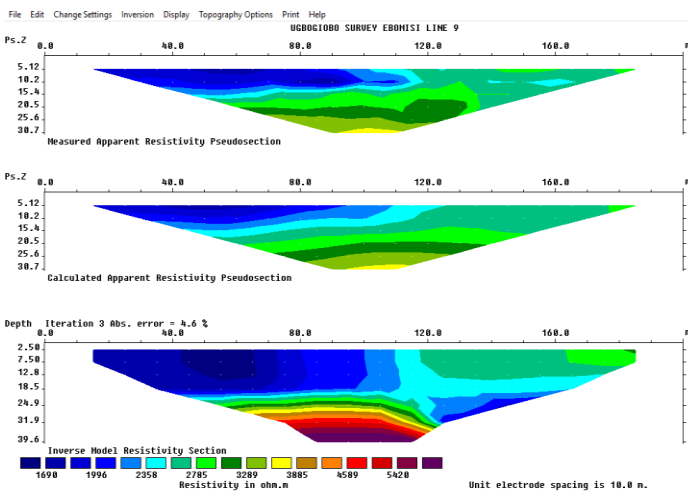


Figure 11: Inverted 2-D resistivity imaging model obtained from Ugbogiobo community profile nine

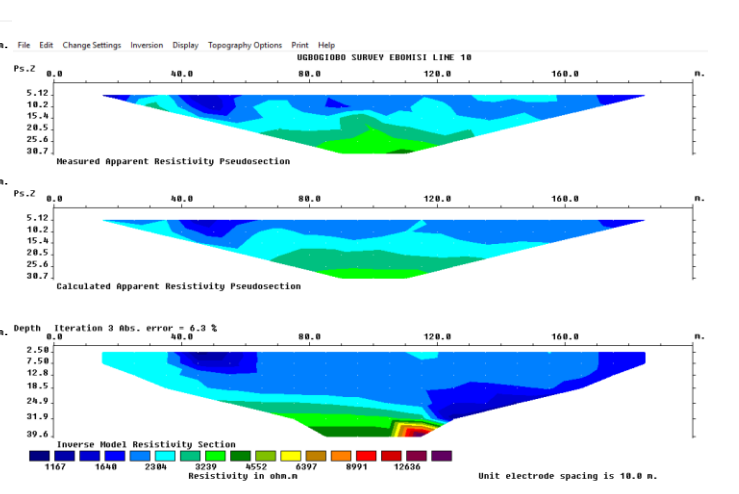


Figure 12: Inverted 2-D resistivity imaging model obtained from from Ugbogiobo community profile

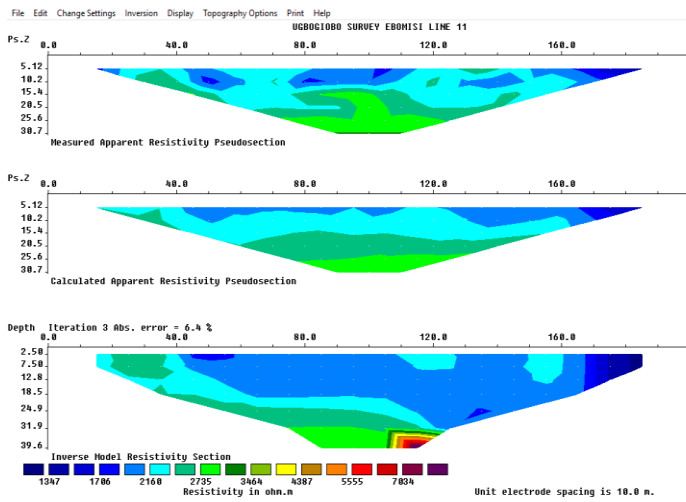


Figure 13: Inverted 2-D resistivity imaging model obtained from Ugbojiobo community profile eleven

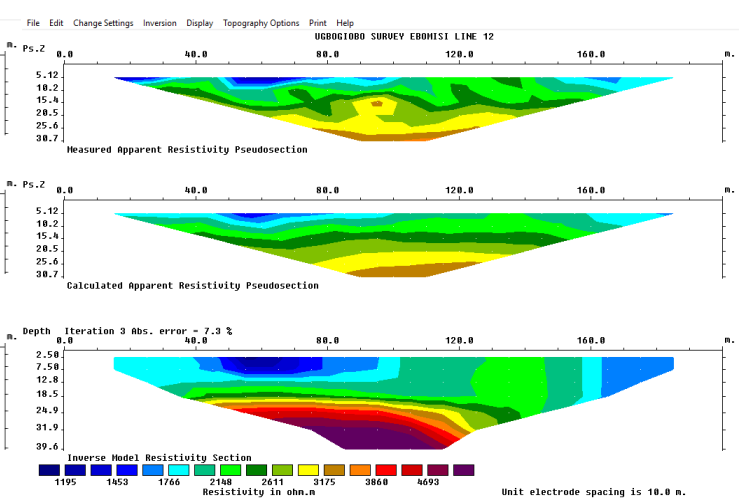


Figure 14: Inverted 2-D resistivity imaging model obtained from Ugbojiobo community profile twelve

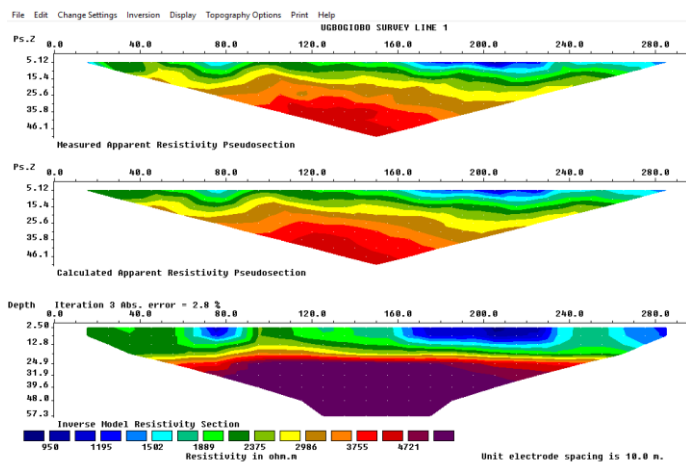


Figure 15: Inverted 2-D resistivity imaging model obtained from Ugbojiobo community profile thirteen

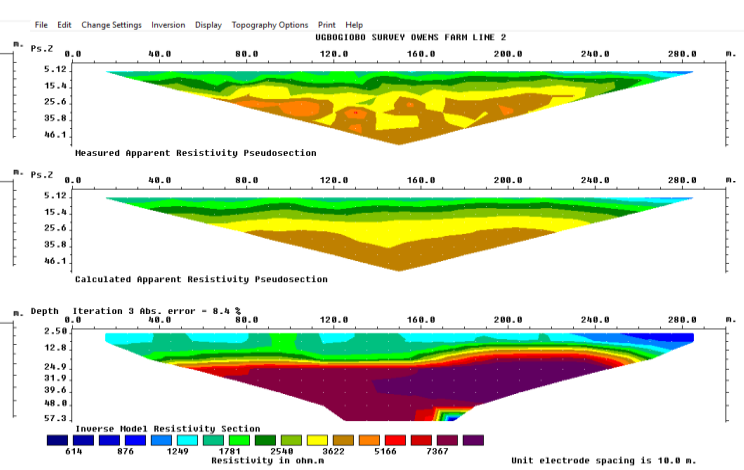


Figure 16: Inverted 2-D resistivity imaging model obtained from Ugbojiobo community profile fourteen

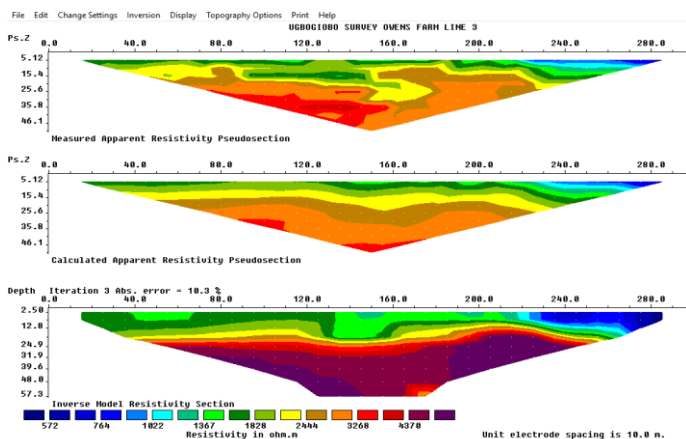


Figure 17: Inverted 2-D resistivity imaging model obtained from community profile fifteen

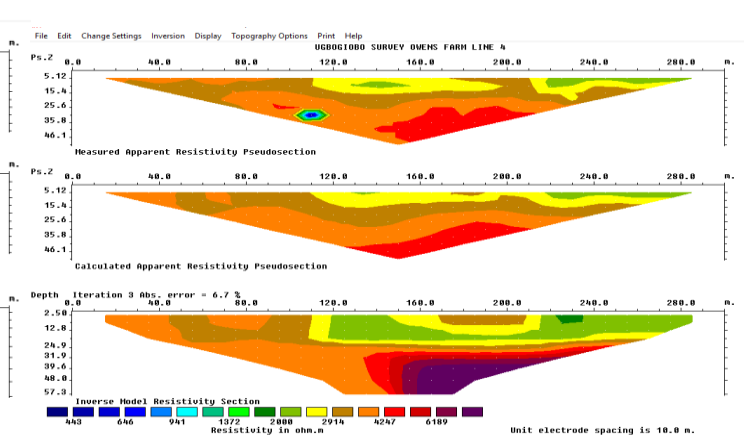


Figure 18: Inverted 2-D from Ugbojiobo community profile obtained from community profile sixteen

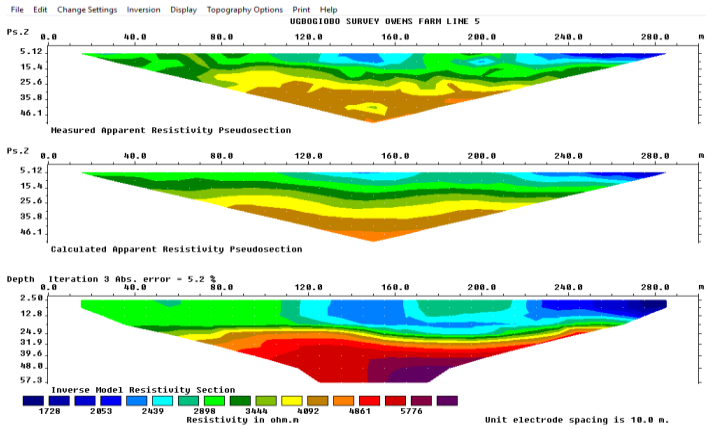


Figure 19: Inverted 2-D resistivity imaging model obtained from Ugbogiobo community profile

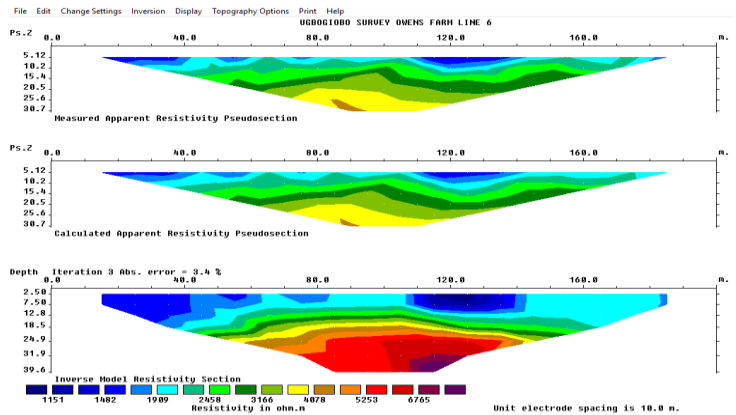


Figure 20: Inverted 2-D resistivity imaging model obtained from Ugbogiobo community profile eighteen

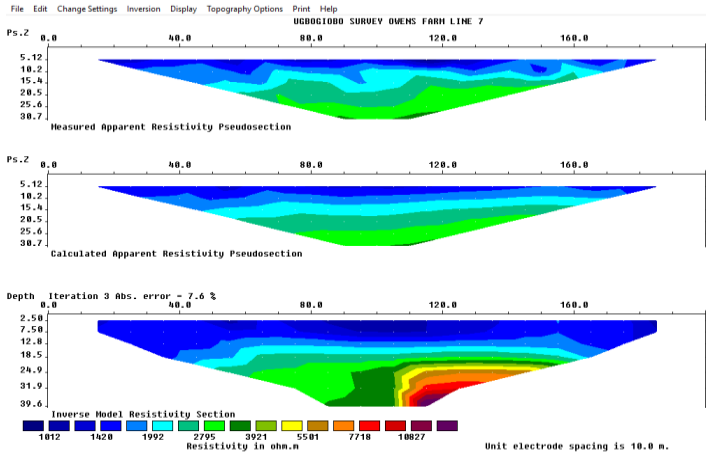


Figure 21: Inverted 2-D resistivity imaging model Obtained from Ugbogiobo community profile twenty nineteen

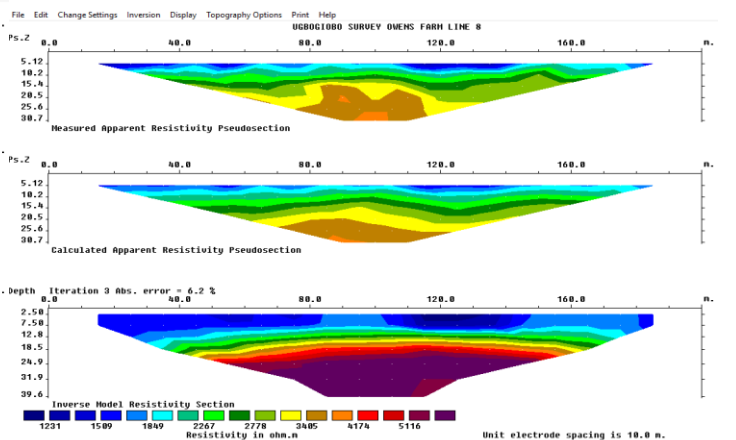


Figure 22: Inverted 2-D resistivity imaging model obtained from Ugbogiobo community profile twenty

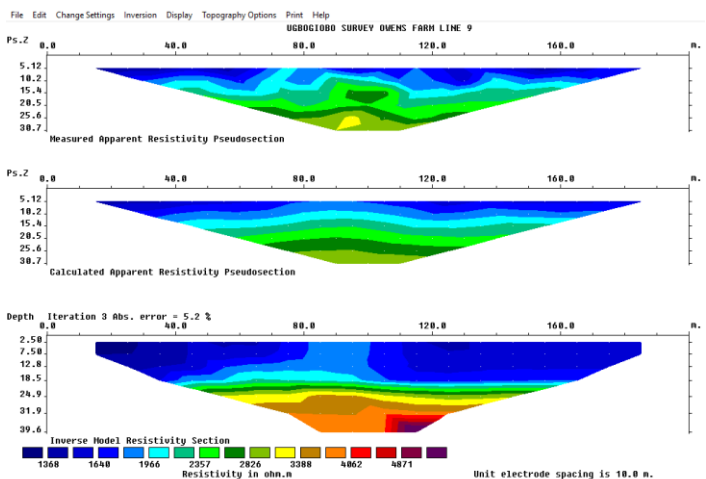


Figure 23: Inverted 2-D resistivity imaging model Obtained from Ugbogiobo community profile twenty one

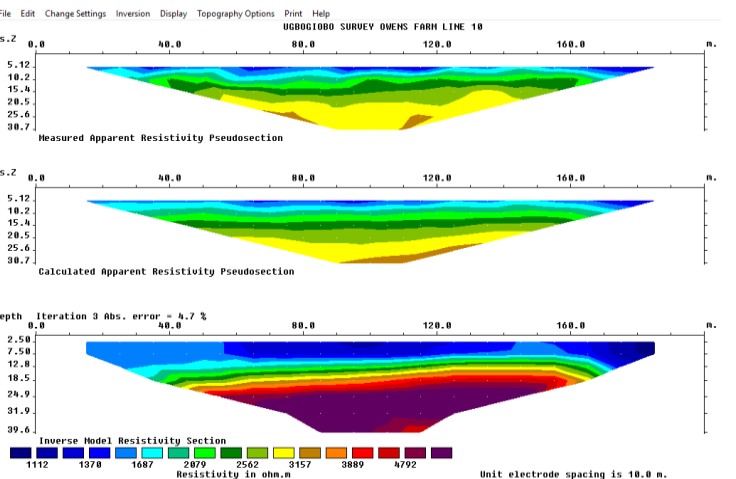


Figure 24: Inverted 2-D resistivity imaging model obtained from Ugbogiobo community profile twenty-two

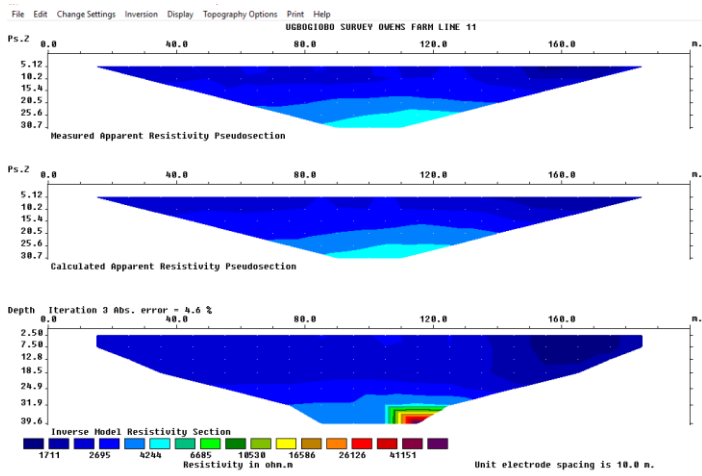


Figure 25: Inverted 2-D resistivity imaging model obtained from Ugbogiobo community profile twenty-three

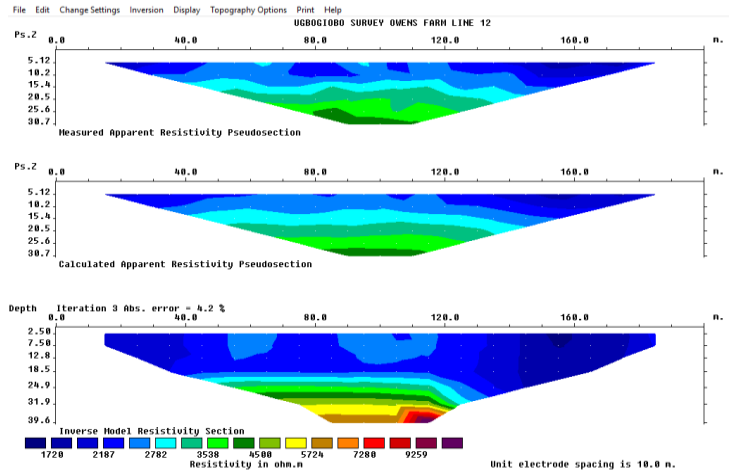


Figure 26: Inverted 2-D resistivity imaging model obtained from Ugbogiobo community profile twenty-four

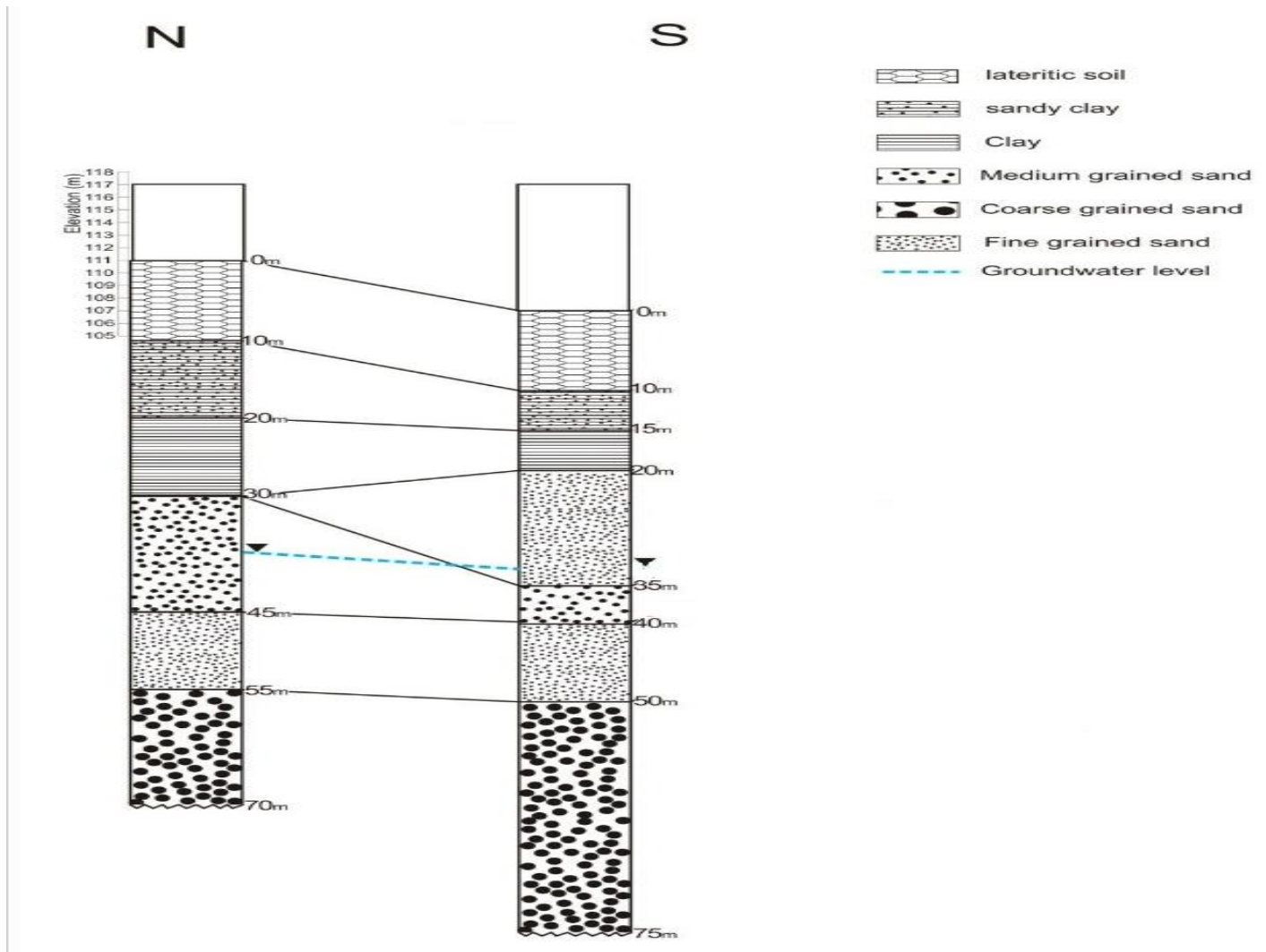


Figure 27: Lithologic section of the study area and environ.

Table 1: Summary of subsurface formation results from the 12 transverses for both locations.

S/N	TRANSVERSE	LENGHT (m)	LAYERS	DEPTH RANGE (m)	RES RANGE (Ω m)	INTERPRETATION
1	TRNSV 01	300	8	2.50-57.30	1315-6190	Alluvium soil, clayey soil, shale Stand stone
2	TRNSV 02	300	5	2.50-57.30	13.69-9413	Limestone, clay soil, sand stone, shale and thick clay
3	TRNSV 03	300	4	2.50-57.30	837-6199	Alluvium soil, clay soil, Thick clay
4	TRNSV 04	300	4	2.50-57.30	1775-8631	Alluvium, clay soil. Thick clay.
5	TRNSV 05	300	5	2.50-57.30	1315-6146	Alluvium, clay soil, sand stone, Shale, thick clay
6	TRNSV 06	200	5	2.50 – 39.6	1125-9178	Alluvium soil, clayey soil, sandstone, limestone Shale
7	TRNSV 07	200	6	2.50-39.6	1116 – 5818	Alluvium soil, clayey soil, limestone, sandstone, shale
8	TRNSV 08	200	5	2.50 -39.6	1507 - 7970	Alluvium soil, sandstone, clayey soil. Shale, limestone
9	TRNSV 09	200	6	2.50 – 39.6	1690 - 5420	Alluvium soil, clay soil, limestone, shale, sandstone, shale.
10	TRNSV 10	200	6	2.50 – 39.6	1167 -12638	Alluvium soil, sandstone, thick clay, limestone, shale.
11	TRNSV 11	200	4	2.50-39.6	1347-7834	Alluvium soil, sandstone, thick clay, limestone, shale.
12	TRNSV 12	200	5	2.50-39.6	1195-4693	Alluvium soil, clay soil, sandstone, thick clay, limestone, shale.
13	TRNSV 13	300	6	2.50-57.3	950-4721	sandstone, shale, limestone.
14	TRNSV 14	300	4	2.50-57.3	614-7367	clayey soil, sandstone, thick clay, limestone.
15	TRNSV 15	300	5	2.50-57.3	572-4370	clayey soil, sandstone, thick clay, limestone, shale.
16	TRNSV 16	300	6	2.50-57.3	443-6189	clayey soil, sandstone, thick clay, limestone.
17	TRNSV 17	300	5	2.50-57.3	1728-5776	clayey soil, sandstone, thick clay, limestone, shale.
18	TRNSV 18	200	5	2.50-39.6	1151-6765	clayey soil, sandstone, thick clay, limestone.
19	TRNSV 19	200	5	2.50-39.6	1012-10827	clayey soil, sandstone, thick clay, limestone.
20	TRNSV 20	200	6	2.50-39.6	1231-5116	clayey soil, sandstone, thick clay, limestone, shale.
21	TRNSV 21	200	5	2.50-39.6	1368-4871	clayey soil, sandstone, limestone, shale.
22	TRNSV 22	200	5	2.50-39.6	1112-4792	clayey soil, sandstone, limestone, shale.
23	TRNSV 23	200	3	2.50-39.6	1711-41154	clayey soil, sandstone, thick clay, limestone, shale.
24	TRNSV 24	200	4	2.50-39.6	1720-9259	clayey soil, sandstone, thick clay, limestone, shale.

7.0 CONCLUSION

Geophysical investigations using 2D electrical imaging consisting of 24 traverses were carried out in two locations in Ugbogiobo community of Ovia North East Local Government Area of Edo State, Nigeria for subsurface classification in the study area. Twenty-Four profiles were taken in the study area making it twelve profiles in each location which form the 2D Electrical Resistivity Imaging (ERI) using the Wenner array.

It is evident from the result of the modelled 2D images that the Lithology of the area is seen to have some buried rocks materials and minerals over a depth between 2.5 m to 57.3 m for all the profiled lines which reveals the composition of Alluvium and clayey soil at the top surface with low resistivity values at a depth below 10 m, while Shale, Slate, Sandstone falls at a depth between 13 m to 25 m and below a depth of 50 m, marble can be inferred. Although the standard resistivity value shows an occurrence of hard rock (Igneous and metamorphic rock), which ranges from 30m to 56m below. However, the lithological profile of the existing borehole data obtained in the study area shows that the formations from 0m-70m are sedimentary beds of sandstone, clay and clayey soil. Therefore, the high resistivity value is occasioned by the presence of stratified sand stone and thick clay layers encountered about 30m as shown in the litholog presented in figure 27.

REFERENCES

- [1] Alile, O. M. and Abraham, E. M. "Three-dimensional Geoelectrical Imaging of the Subsurface Structure of University of Benin-Edo state Nigeria". *Advances in Applied Science Research*, 6(11), 2015, 85-93.
- [2] Badmus, B.S., Akinyemi, O.D., Olowofela, J.A. and Folarin, G.M. "3D Electrical Resistivity Tomography Survey for the Basement of the Abeokuta Terrain of Southwestern Nigeria". *Journal of Geological Society India*, 80, 2012, 845. <https://doi.org/10.1007/s12594-012-0213-x>.
- [3] Abdelwahab, H. "Comparison of 2D and 3D resistivity imaging methods in the study of shallow subsurface structures". *Greener Journal of Physical Sciences*, 3(4), 2013, 149-158.
- [4] Aizebeokhai, A.P. and Singh, V.S. "Field Evaluation of 3D Geoelectrical Resistivity Imaging for Environmental and Engineering Investigations Using Parallel 2D Profiles". *Current Science*, 105(4), 2013, 504-512.
- [5] Ogunsanwo, O. "International Association of Engineering Geology Bulletin", 131-135, 1989.
- [6] Short, K.C. and Stauble, A.J. "Outline of Geology of Niger Delta": *AAPG Bulletin*, 51, 19677, 61-779.
- [7] Erah, P.O., Akujieze, C.N. and Oteze, G.E. "Tropical Journal of Pharmaceutical Research", 1(2), 2002, 75 - 82.
- [8] Kogbe, C.A. "Geology of Nigeria. Rock View (Nig.) Ltd.", *First published 1975*, 1989, 39-56.
- [9] Alile, O.M., Ujuanbi, O. and Evbuomwan, I.A. "Geoelectrical Investigation of Groundwater in Obaretin-Iyanomon Locality". *Journal of Geological Mineral Resources*, 3(1), 2011, 13 - 20.
- [10] Loke, M.H. and Barker, R.D. "Rapid Least Squares Inversion of Apparent Resistivity Pseudosections by a Quasi-Newton Method." *Geophysical Prospecting*, 44, 1996b, 131-152.
- [11] Kearey, P., Michael, B. and Ian, H. An Introduction to Geophysical Exploration. Blackwell Science, Limited, Oxford, U.K. 2002, 257.
- [12] Griffiths, D.H. and Barker, R.D. Two-dimensional Resistivity Imaging and Modeling in Areas of Complex, 1993.
- [13] Loke, M.H. and Barker, R.D. "Practical techniques for 3D resistivity surveys and data inversion." *Geophysical Prospecting*, 44, 1996a, 499-523.